

Formation, Spatiotemporal Dynamics, and Control of Structures in Weakly Developed Drift Wave Turbulence^{*)}

Olaf GRULKE^{1,2)}, Thomas WINDISCH¹⁾, Christian BRANDT¹⁾,
Stefan ULLRICH¹⁾ and Thomas KLINGER^{1,2)}

¹⁾*MPI for Plasma Physics, EURATOM Association, 17491 Greifswald, Germany*

²⁾*Ernst-Moritz-Arndt University, 17489 Greifswald, Germany*

(Received 2 September 2008 / Accepted 8 December 2009)

Experimental investigations of the evolution of the dynamics of drift wave turbulence in a linear high-density helicon plasma device are presented. The turbulent density fluctuations in the plasma edge are characterized by large intermittent events caused by radially propagating turbulent structures, which are formed in the radial plasma density region due to increased cross-field transport by a quasi-coherent drift wave mode. Similar to coherent drift wave modes the turbulent structures are correlated with fluctuating parallel currents. The role of fluctuating currents parallel to the ambient magnetic field in the evolution of coherent drift wave modes and drift turbulence is highlighted by investigations of the interaction of drift wave fluctuations with externally driven currents. Frequency pulling of coherent drift wave modes over a frequency range of up to 30% of the natural drift wave frequency is demonstrated. Furthermore, the drive of mode-selective current patterns allow for complete synchronization of drift wave turbulence and consequently leads to a strong reduction of the associated fluctuation-induced transport.

© 2010 The Japan Society of Plasma Science and Nuclear Fusion Research

Keywords: laboratory plasma, drift wave turbulence, turbulent structures, turbulence control

DOI: 10.1585/pfr.5.013

1. Introduction

Fluctuations in plasma turbulence display a strong intermittent character with sporadic large fluctuation events [1–4]. Those events are ascribed to the occurrence of transient large-scale structures, which form within the turbulent fluctuation, most likely due to inverse energy cascading processes, propagate and decay. Due to their large-scale nature turbulent structures have been subject of intense investigations in the context of fluctuation-induced, the so-called anomalous, transport processes. The paradigm of the mechanism of the fluctuation-induced transport is the passive convection of plasma within potential vortices [5]. The large-scale structures are particularly important for this process because their large spatial extent determines the spatial transport scales. Improved diagnostics in the scrape-off layer (SOL) of tokamaks revealed that in addition to the convection in potential vortices cross-field transport is also caused by the direct radial propagation of large density fluctuation structures over distances larger than the typical structure size [6–8], thereby affecting key fusion experiment issues like heat deposition on the first wall and first wall recycling. It was shown that the radial propagation of turbulent structures can cause up to 30% of the total radial transport [9]. In a fundamental model approach the radial structure propagation in the

tokamak SOL is explained by polarization of density fluctuation structures due to curvature and ∇B -drifts [10, 11]. Extended models show that the formation and radial propagation of structures is a result of the dominance of interchange mode dynamics in the tokamak SOL [12, 13]. The self-consistent azimuthal electric field of the structures results in a radially outwards $E \times B$ drift, which cause radial structure propagation and large transport events in the far-SOL [14]. The characteristic electric field pattern has been experimentally confirmed [15]. The situation is much less clear in the tokamak edge plasma, which forms the interface between the hot plasma core and the SOL. Numerical simulations demonstrated that in the tokamak edge the turbulent fluctuations are caused by the drift wave instability [16]. The very limited diagnostic access of the edge plasma on the spatial and temporal scales of the turbulent fluctuations makes a characterization of the structure dynamics extremely difficult. However, fundamental studies of predominantly the electrostatic drift wave instability and electrostatic drift wave turbulence have intensely been done in laboratory plasmas [17–23]. It has been demonstrated that the formation of turbulent structures is a generic feature of drift wave turbulence. This paper deals with experimental investigations of the dynamics of structures in drift wave turbulence as observed in a cylindrical linear laboratory plasma device. In Sec. 2 the device and chief diagnostic tools are described. Section 3

author's e-mail: Grulke@ipp.mpg.de

^{*)} This article is based on the invited talk at the 14th International Congress on Plasma Physics (ICPP2008).

deals with the formation and characterization of the dynamics of turbulent structures. The role of parallel plasma currents in the evolution of the fluctuations is highlighted in Sec. 4. In Sec. 5 the influence of externally driven currents on the turbulent dynamics is studied before the results are summarized in Sec. 6 and conclusions are drawn.

2. Experimental Setup and Diagnostics

The experiments are carried out in the linear cylindrical experiment VINETA [24]. A schematic of the device and major diagnostics is shown in Fig. 1. It consists of an $L = 4.5$ m long vacuum vessel with a diameter of $D = 0.4$ m immersed in a set of 36 magnetic field coils, which generate a maximum steady-state homogeneous magnetic field of $B = 0.1$ T. Plasma is generated by non-resonant helicon wave heating. At one end of the device the helicon source is located. The source consists of an $m = 1$ helicon antenna wrapped around a Pyrex glass extension with an inner diameter of $d = 0.1$ m. The source is operated at a rf frequency of $f_{\text{rf}} = 13.56$ MHz and a rf power of typically $P_{\text{rf}} \leq 4$ kW. As a characteristics of helicon discharges a high density plasma is generated with a peak plasma density of $n \leq 2 \cdot 10^{19} \text{ m}^{-3}$, although at a low electron temperature of $T_e \approx 3$ eV. The radial plasma density profile is peaked in the plasma center and has a nearly Gaussian shape [25]. Due to the high plasma density at small electron temperature the plasma is characterized by high collisionality. The electron-ion collision frequency ω_{ei} in the plasma center is much larger than the ion cyclotron frequency ω_{ci} , typically $\omega_{ei}/\omega_{ci} \leq 100$. Although some experimental results indicate a strong neutral gas depletion in the plasma center [26], the edge plasma is characterized by a high electron-neutral collision frequency, which is of similar order or even larger than ω_{ei} . The plasma potential has a maximum in the plasma center and decreases radially. Due to the almost parabolic shape of the radial plasma potential profile in the central region the associated azimuthal $E \times B$ velocity leads to

an almost rigid body rotation of the plasma opposite to the electron diamagnetic drift direction. However, in the plasma edge the $E \times B$ velocity has a radial shear [27]. The main diagnostic tools for the measurements of time-averaged plasma profiles and fluctuations are probes. Evaluation of the characteristics of Langmuir probes, which are compensated against rf fluctuations, using a kinetic probe theory [28] yields the time-averaged plasma parameters as plasma density, electron temperature, and plasma potential. Plasma parameter profiles are obtained using various high precision probe positioning systems, which are also depicted in Fig. 1. Radial plasma density profiles are calibrated against a 160 GHz heterodyne microwave interferometer. Fluctuations of the plasma density are measured by negatively biased Langmuir probes, assuming electron temperature fluctuations to be negligible. The probes are used as single probes or one-dimensional probe arrays, covering an azimuthal plasma circumference or a vertical cut through the plasma. Fluctuations of the plasma potential are diagnosed by measurements of floating potential fluctuations. The reliability of this approach has been validated by comparing the floating potential fluctuations with plasma potential fluctuations measured by a novel laser-heated emissive probe [29]. For measurements of magnetic field fluctuations highly sensitive 3 axes induction probes in orthogonal arrangement are used, which are compensated against electrostatic pickup. The amplitude response and the respective relative spatial position of the induction probes are calibrated in a magnetic test field.

To reconstruct the fluctuations characteristics in a two-dimensional plasma cross sections, correlation analysis and conditional averaging [30] is performed between a reference probe and a scanning probe in a series of reproducible consecutive plasma discharges. The scanning probe is either a single probe or a one-dimensional probe array. In the case of conditional averaging an amplitude condition on the reference signal is chosen in order to extract the large-amplitude fluctuation pattern. This procedure is performed for plasma density, plasma potential, and magnetic field fluctuations.

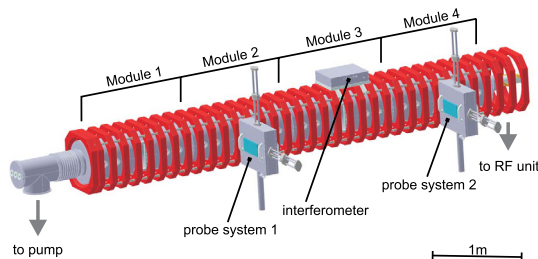


Fig. 1 Schematic of the VINETA device. The helicon source setup is located on the right hand side end of the device. Additionally, major diagnostic tools as the probe positioning systems and the microwave interferometer are also shown.

3. Dynamics of Structures in Drift Wave Turbulence

It was demonstrated that the radial plasma density gradient gives rise to the drift wave instability [23]. By changing the ambient magnetic field single drift wave modes can be destabilized with mode numbers ranging from $m = 1, \dots, 9$. The drift wave mode structures and frequencies agree well with linear dispersion calculations [31], which also show that the radial mode structure is strongly influenced by the radial gradient of collision frequency leading to azimuthally bent eigenmode structures. For increasing ambient magnetic field the drift wave modes undergo a series of mode coupling phenomena, which leads to a weakly developed turbulent state [21]. Bicoherence

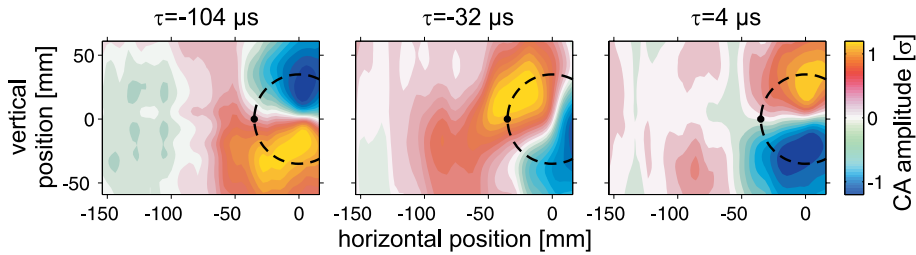


Fig. 2 Conditionally averaged density fluctuations in the azimuthal plane with for weakly developed drift wave turbulence. The black dot marks the position of the reference probe. The dashed circle indicates the position of the maximum radial density gradient.

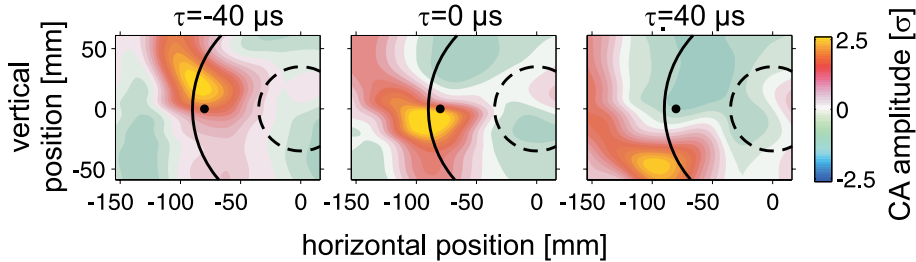


Fig. 3 Conditionally averaged density fluctuations in the azimuthal plane with for weakly developed drift wave turbulence. The black dot marks the position of the reference probe. The solid circle indicates the azimuthal direction.

analysis demonstrated the dominance of a quasi-coherent $m = 1$ drift mode within the turbulent fluctuations most likely as a result of an inverse energy cascade [32]. The inverse energy cascade seems to be a generic feature of drift wave turbulence in linear magnetic geometry and has been suggested to be important in the evolution of an $m = 0$ mode [33]. Conditionally averaged density fluctuations in an azimuthal cross section with respect to density fluctuations in the maximum radial plasma density gradient acting as reference signal for three time instants $\tau = -104, -32, 4 \mu\text{s}$ are shown in Fig. 2. Only density fluctuations are considered as reference, which amplitude exceed 2σ , where σ is the standard deviation of the entire fluctuation time series. In the radial plasma density gradient region the propagation of a quasi-coherent $m = 1$ drift mode like structure is observed. The propagation is purely azimuthal in direction of the electron diamagnetic drift. The fluctuation-induced cross-field transport caused by the quasi-coherent $m = 1$ mode leads to radial transport of high plasma density. This is visible for $\tau = -32 \mu\text{s}$ in Fig. 2. A package of high plasma density peels off the quasi-coherent mode and is radially transported into the plasmas edge region. In the plasma edge the time-averaged azimuthal $E \times B$ drift exceeds the electron diamagnetic drift and accordingly the density package propagates into opposite direction, c.f. Fig. 2, $\tau = 4 \mu\text{s}$. The dynamics of density fluctuations in the plasma edge is investigated by repeating the conditional averaging procedure with respect to edge plasma density fluctuations, Fig. 3. Shown are conditionally averaged density fluctuations in the same representation as in Fig. 2 for the time instants $\tau = -40, 0, 40 \mu\text{s}$.

In contrast to the propagation of the quasi-coherent drift wave mode (Fig. 2) the turbulent structure propagates azimuthally into opposite direction with $E \times B$ velocity. However, the propagation is not purely azimuthal but the structure has also a radial component of propagation, which leads to a radial displacement during its lifetime. A quantitative analysis revealed that the radial velocity is only 30% of the structure's azimuthal propagation speed [27]. In normalized units the radial propagation velocity is approx. 10% of the local ion sound speed, which is comparable to the situation in the tokamak SOL. The cause for the radial propagation is apparent if the associated potential fluctuation structure is measured. In Fig. 4 measured equipotential contours are superimposed for the case of the quasi-coherent mode in the radial plasma density gradient region and the turbulent structure in the plasma edge. In contrast to a strictly coherent drift wave mode the phase shift between density and potential fluctuations is large with approx. $\pi/2$. This results in a large radial transport, which leads to the occurrence of a high density structure in the edge plasma. This structure has also a potential pattern, which is azimuthally phase shifted to the density pattern and results in a radial $E \times B$ drift. The amplitude of edge density fluctuations is comparable to the time-averaged plasma density in the maximum radial density gradient region [27], which supports that indeed turbulent structures in the plasma edge originate in the quasi-coherent drift wave region. The fundamental mechanism for radial propagation is thus identical to tokamak SOL situation: Due to the turbulent dynamics the self-consistent plasma potential fluctuations are phase shifted to the den-

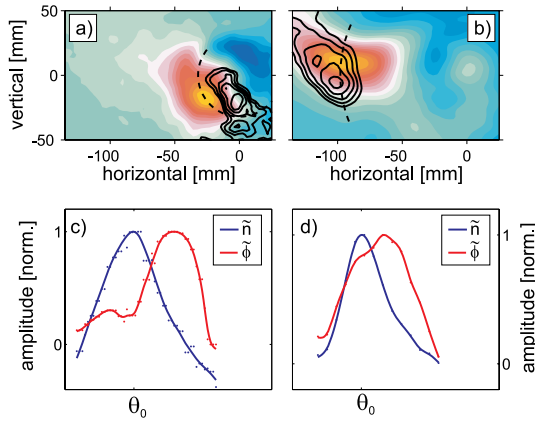


Fig. 4 Conditionally averaged density fluctuation structure with superimposed contour plot of the associated positive potential fluctuation in the radial plasma density gradient region (a) and the plasma edge (b). Additionally, a cut through the center of the structures indicated as dashed lines in (a) and (b) is shown in (c) and (d), respectively.

sity fluctuations. The associated azimuthal electric field causes a radially outwards $E \times B$ drift, which leads to radial structure propagation. However, the details of the generation of the phase-shifted potential fluctuation is different. It has been shown in experimental investigations [9, 15] and numerical simulations [13, 34] that in the tokamak SOL the turbulent fluctuations are governed by interchange mode dynamics, which strongly relies on the curvature of the magnetic field. This mechanism is absent in the present experiment configuration.

4. Parallel Flux of Turbulent Fluctuations

The main ingredient in the evolution of the drift wave instability and drift wave turbulence is the electron flow parallel to the ambient magnetic field in response to the plasma pressure fluctuations. The associated currents are an intrinsic feature also of electrostatic drift waves, although here induction does not significantly affect the non-adiabaticity of the electrons. Measurements of magnetic field fluctuations using the induction probe diagnostics yield information about the associated current pattern. In the case of strictly coherent fluctuations the current pattern can reliably be reconstructed. An example of the current for a specific phase of a coherent $m = 2$ drift wave mode is shown in Fig. 5. In total four current channels are observed, two channels with current directed along the ambient magnetic field and two directed oppositely. The peak absolute current for both current directions is $j_{\parallel} \approx 100 \text{ mA/cm}^2$. Similar to the potential fluctuations of the coherent drift mode no phase shift is observed between the mode's density fluctuations and fluctuating parallel currents. The currents strictly track the density fluctua-

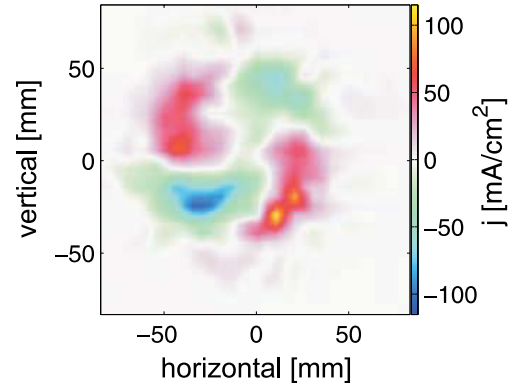


Fig. 5 Parallel current pattern associated with a coherent $m = 2$ drift wave mode.

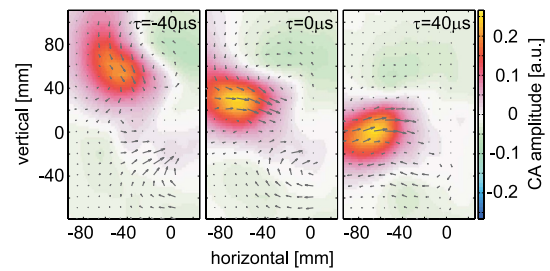


Fig. 6 Conditionally averaged magnetic field fluctuation pattern (arrows) associated with a propagating turbulent density structure in the plasma edge.

tations during the azimuthal mode propagation. A similar investigation is done for the radially propagating turbulent structures in the plasma edge. The conditionally averaged magnetic field fluctuations are measured with respect to large-amplitude edge density fluctuations. The results of the measurement are depicted in Fig. 6. Shown are the conditionally averaged density fluctuations in an azimuthal cross section together with two components of the magnetic field fluctuations. Both signals are extracted using the same reference signal and condition. Very similar to Fig. 3 a turbulent structure develops and shows a mainly azimuthal propagation with time-averaged $E \times B$ drift. The density fluctuation structure displays a correlation with magnetic field perturbations, shown in Fig. 6 as arrows. At the time instant $\tau = -40 \mu\text{s}$ the turbulent density structure has formed. At the same time the magnetic signature of a current filament is observed. The maximum amplitude of the magnetic field fluctuations is located mainly at the position of the density structures. This finding holds true during the entire lifetime of the density structure. In contrast to the coherent drift wave mode this result demonstrates that the current filament is not located at the position of the maximum density fluctuation but is phase shifted azimuthally by approx. $\pi/2$. As the density structure propagates azimuthally the magnetic field perturbations move also azimuthally and the phase shift to the density pattern

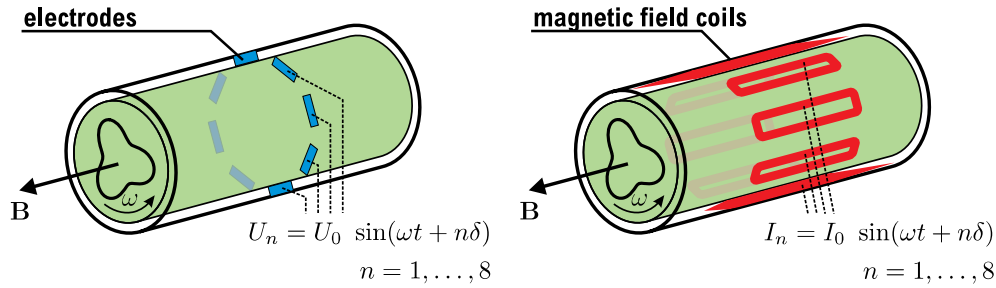


Fig. 7 Schematic of the experimental instruments to drive parallel plasma currents mode-selectively: electrode exciter (left) and inductive exciter (right).

persists. The details of the phase relation between density and parallel plasma current is subject of further investigations. However, this finding clearly demonstrates that also in the plasma edge density fluctuations are associated with fluctuating parallel plasma currents, comparable to the coherent drift wave mode, and shows that the dynamics of the radially propagating turbulent structures is intrinsically three-dimensional. This finding represents the major difference to the radially propagating structures in the tokamak SOL, where the quasi two-dimensional interchange mode dynamics dominates.

5. Interaction of Fluctuations with Driven Parallel Currents

The correlation of the fluctuating plasma currents parallel to the ambient magnetic field on the evolution of the coherent drift wave modes and radially propagating structures in drift wave turbulence strongly suggests that both dynamical states can be influenced by externally driving the plasma currents. A study of the interaction of coherent drift wave modes with periodically driven Alfvén waves showed non-linear interaction and demonstrated that the drift mode dispersion can be altered due to the presence of the Alfvén wave [25]. First evidence was obtained that the interaction occurs between the drift mode currents, which are mainly located in the strong radial plasma gradient region, and the Alfvén wave current located in the plasma center. We extend the study by imposing mode patterns of the parallel currents, similar to current pattern of the coherent drift mode itself, by two experimental arrangements, shown in Fig. 7. The first setup consists of 8 azimuthally arranged electrodes, which are in direct contact with the plasma in the outer edge. The electrodes can be biased periodically with a variable phase shift between the individual electrodes. This way an azimuthally rotating current pattern with mode numbers $m \leq 3$ (Nyquist limit) can be generated. The maximum current density amplitude drawn by the electrodes is typically $j_{ex} \leq 1 \text{ A/cm}^2$, which is on the same order of magnitude as the intrinsic drift mode currents (c.f. Fig. 5). The frequency of the mode pattern can be chosen in the range $f_{ex} = 1 \dots 20 \text{ kHz}$,

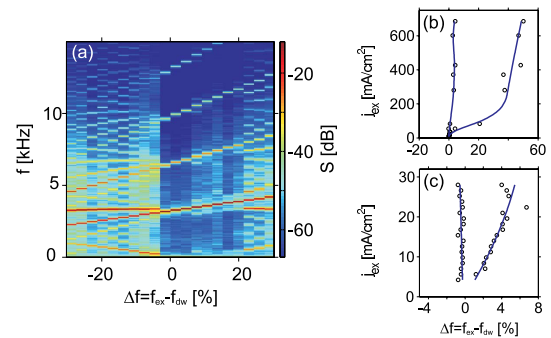


Fig. 8 Interaction of a driven $m = 2$ current pattern with a coherent $m = 2$ drift wave mode. Spectrogram of density fluctuations for a frequency scan of the current pattern as generated by the electrode exciter (a), dependence of the coherent drift mode synchronization range on the amplitude of the driven current density for the electrode exciter (b) and the coil exciter (c).

which covers the frequency range of coherent drift modes in VINETA. The second arrangement consists of a set of 8 magnetic saddle coils surrounding the plasma azimuthally. The coils are connected to audio amplifiers with a maximum output power of 600 W via an impedance network. The impedance matching allows presently for mode frequencies $f_{ex} = 1, \dots, 10 \text{ kHz}$. The details of the experimental setup will be published elsewhere. Due to the inductive drive the coil exciter has no direct plasma contact. The maximum amplitude of driven parallel plasma currents is significantly smaller when compared to the electrode exciter with typically $j_{ex} \leq 50 \text{ mA/cm}^2$. First, the influence of the driven current pattern on the dynamics of coherent drift wave modes is studied. For the case of a $m = 2$ drift wave mode a current with the same mode pattern is driven with both exciter setups. The azimuthal phase velocity of the driven current pattern is in direction of the electron diamagnetic drift velocity. The frequency of the current pattern is increased in consecutive discharges across the natural drift mode frequency. The spectral evolution of density fluctuations is shown in Fig. 8(a). The drift wave mode has a frequency of $f_{dw} = 3 \text{ kHz}$ and in

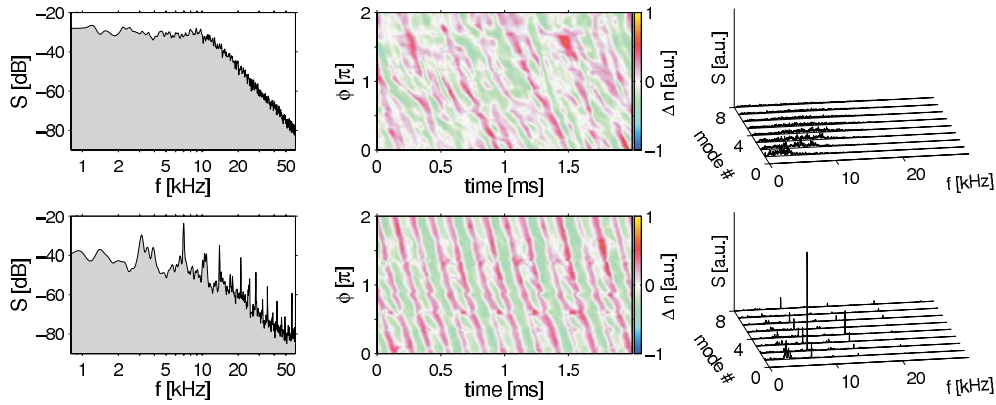


Fig. 9 Power density spectra (left), time series of density fluctuations along an azimuthal plasma circumference (middle), and corresponding wavenumber-frequency spectra (right) for weakly developed drift wave turbulence (top) and synchronization of turbulence with the electrode exciter (bottom).

this case the electrode exciter is scanned in frequency in the range $f_{\text{ex}} = 2, \dots, 4$ kHz. The drift wave mode and exciter fluctuation co-exist until the exciter frequency approaches the drift mode frequency. This is not only visible for the fundamental frequency but also for the higher harmonics. When the exciter frequency approaches the drift wave mode frequency, the mode is synchronized by the driven current pattern and is dragged in frequency until a frequency mismatch of approx. 20%. At this point the drift mode is found independently of the exciter signal at exactly the natural drift wave mode frequency of $f_{\text{dw}} = 3$ kHz. The frequency range, in which synchronization is observed, is not symmetric to the natural drift mode frequency but is mainly achieved if the exciter frequency is larger than the natural mode frequency. The range of mode synchronization is not fixed but has a dependence on the amplitude of the driven currents. In Fig. 8 the frequency range of synchronization in dependence of the amplitude of the driven plasma current is shown for the electrode exciter (b) and the coil exciter (c). For all amplitudes it is again found that synchronization is mainly achieved for higher exciter frequencies. The range of synchronization increases, however, with increasing amplitude. This is best seen for the case of the electrode exciter, for which the maximum amplitude of the driven currents exceeds the intrinsic drift mode currents (c.f. Fig. 5). For an amplitude of $j_{\text{ex}} \leq 20$ mA/cm² the frequency range of synchronization increases almost linearly with amplitude. For higher amplitudes a strongly non-linear increase is observed until the increase in frequency range saturates at $j_{\text{ex}} \approx 200$ mA/cm² at a frequency mismatch of 30%. A similar behavior is observed for the inductive exciter. Here, the current amplitudes are much smaller with $j_{\text{ex}} \leq 30$ mA/cm² and only the linear increase of synchronization range is observed. The observed dependence of synchronization on the amplitude of the control signal is a characteristic feature of nonlinear systems and the region of synchronization is called Arnold tongue [35] and strongly suggests the nonlinear character

of the interaction of the drift wave mode currents and the externally driven currents. It is interesting to note that for synchronization the amplitude of the driven current can be as small as 5% of the intrinsic drift wave mode currents. Synchronization is only observed if the phase velocity of the driven current pattern is in direction of the phase velocity of the drift wave mode. If the current pattern propagates into the opposite direction no synchronization is observed at all. The strong influence of the driven currents on the dispersion of coherent drift wave modes strongly motivates to apply the same strategy as a control system for the drift wave turbulence state. Figure 9 compiles the features of turbulent density fluctuations. The power density spectrum shows no pronounced drift wave mode peak and follows a power law decrease for frequencies $f \geq 10$ kHz. The non-coherent behavior is also visible in the time series of density fluctuations measured simultaneously in the radial density gradient region along an azimuthal plasma circumference. The fluctuations are irregular and show frequent phase jumps. The corresponding wavenumber-frequency spectrum is flat without any dominant modes. If we drive a $m = 2$ current pattern with the electrode exciter the characteristic turbulent features of density fluctuations alter considerably. The power density spectrum is peaked at a frequency of $f = 7$ kHz and higher harmonics. The density fluctuation time series are regular and show the signature of an $m = 2$ drift wave mode. This is confirmed by the wavenumber-frequency spectrum, which is strongly peaked at a modenummer of $m = 2$. The mode is strictly coherent. It disappears if the exciter current is switched-off and the fluctuations relay to the original turbulent state. Similar to the coherent mode investigations synchronization of turbulence is only observed if the current pattern is propagating parallel to the drift mode phase velocity. Otherwise no influence on the turbulent fluctuations is obtained. A similar behavior was observed in an independent study [36], for which a good agreement with numerical simulations could be achieved. An important

aspect of the synchronized state is that the resulting coherent fluctuations resemble very much a coherent drift wave mode. It is particularly found that in contrast to the turbulent fluctuations the phase shift between density and potential fluctuations is small. Thus, the anomalous transport is significantly reduced in the synchronized turbulence state. Furthermore, the intermittence in the plasma edge is strongly reduced in response to the decreased radial transport.

6. Summary and Conclusions

Investigations of the dynamics of fluctuations in drift wave turbulence in a high-density, homogeneously magnetized helicon plasma device have been presented. The dynamics of the fluctuations in the radial density gradient region and the plasma edge must be distinguished. In the gradient region the fluctuations are dominated by a quasi-coherent drift wave mode, which propagates in electron diamagnetic drift direction. In contrast to a coherent mode the associated plasma potential fluctuations show a large azimuthal phase shift of $\pi/2$ with respect to the density fluctuations. Thus, the radial transport by the quasi-coherent mode is considerably higher, which produces large density fluctuations in the plasma edge region. Those fluctuations propagate azimuthally in opposite direction with time-averaged $E \times B$ drift. Additionally, the associated potential fluctuations cause a radially outwards $E \times B$ drift, which leads to radial propagation of the turbulent structure. This behavior is similar to structures observed in the tokamak SOL. However, measurements of the magnetic field fluctuations revealed that a fluctuating parallel plasma current is correlated with the turbulent density structures in the plasma edge, which indicates the intrinsic three-dimensional dynamics of the structures. This finding represents a major difference to the situation in the tokamak SOL, where the fundamental dynamics is quasi two-dimensional. In contrast to coherent drift wave modes the current is phase shifted with respect to the density fluctuations. The importance of the parallel plasma current is highlighted by the investigation of the interaction of the drift wave fluctuations with externally driven plasma currents. With two different exciter setups, an electrode exciter with direct contact to the plasma and an inductive exciter, parallel plasma currents are driven mode-selectively. A coherent drift wave mode can be synchronized in frequency by the driven plasma currents if the same current mode pattern and the same direction of the phase velocity is chosen. The frequency range of synchronization is strongly dependent on the amplitude of the driven current. The range generally increases nonlinearly with current amplitude, which strongly suggests a nonlinear interaction between the intrinsic drift wave mode currents and the externally driven currents. In the case of drift wave turbulence a full synchronization of the turbulent fluctuation to the prescribed mode is achieved. As in the coherent mode

case synchronization is only achieved if the phase velocity of the driven current pattern is in direction of the mode's phase velocity. The regular fluctuations show all characteristics of coherent drift wave modes, particularly the low level of radial transport.

7. Acknowledgement

This work was supported in parts by No. DFG SFB-TR24/A1.

- [1] C. Hidalgo, Plasma Phys. Control. Fusion **37**, A53 (1995).
- [2] J.A. Boedo, D. Rudakov, R. Moyer, S. Krasheninnikov, D. Whyte, G. McKee, G. Tynan, M. Schaffer, P. Stangeby, P. West, S. Allen, T. Evans, R. Fonck, E. Hollmann, A. Leonard, A. Mahdavi, G. Porter, M. Tillack and G. Antar, Phys. Plasmas **8**, 4826 (2001).
- [3] C. Lechte, S. Niedner and U. Stroth, New J. Phys. **4**, 34.1 (2002).
- [4] O.E. Garcia, V. Naulin, A.H. Nielsen and J.J. Rasmussen, Phys. Plasmas **12**, 062309 (2005).
- [5] W. Horton, Rev. Mod. Phys. **71**, 735 (1999).
- [6] J.L. Terry, R. Maqueda, C.S. Pitcher, S.J. Zweben, B. LaBombard, E.S. Marmor, A.Y. Pigarov and G. Wurden, J. Nucl. Mater. **290-293**, 757 (2001).
- [7] S.J. Zweben, D.P. Stotler, J.L. Terry, B. LaBombard, M. Greenwald, M. Muterspaugh, C.S. Pitcher, the Alcator C-Mod Group, K. Hallatschek, R.J. Maqueda, B. Rogers, J.L. Lowrance, V.J. Mastrocola and G.F. Renda, Phys. Plasmas **9**, 1981 (2002).
- [8] S.J. Zweben, R.J. Maqueda, D.P. Stotler, A. Keese, J. Boedo, C.E. Bush, S.M. Kaye, B. LeBlanc, J.L. Lowrance, V.J. Mastrocola, R. Maingi, N. Nishino, G. Renda, D.W. Swain, J.B. Wilgen and the NSTX Team, Nucl. Fusion **44**, 134 (2004).
- [9] J.A. Boedo, D.L. Rudakov, R.A. Moyer, G.R. McKee, R.J. Colchin, M.J. Schaffer, P.G. Stangeby, W.P. West, S.L. Allen, T.E. Evans, R.J. Fonck, E.M. Hollmann, S. Krasheninnikov, A.W. Leonard, W. Nevins, M.A. Mahdavi, G.D. Porter, G.R. Tynan, D.G. Whyte and X. Xu, Phys. Plasmas **10**, 1670 (2003).
- [10] D.A. D'Ippolito, J.R. Myra and S.I. Krasheninnikov, Phys. Plasmas **9**, 222 (2002).
- [11] D.A. D'Ippolito, J.R. Myra, S.I. Krasheninnikov, G.Q. Yu and A.Y. Pigarov, Contrib. Plasma Phys. **44**, 205 (2004).
- [12] O.E. Garcia, V. Naulin, A.H. Nielsen and J.J. Rasmussen, Phys. Rev. Lett. **92**, 165003 (2004).
- [13] D. Russell, D.A. D'Ippolito, J.R. Myra, W.M. Nevins and X.Q. Xu, Phys. Rev. Lett. **93**, 265001 (2004).
- [14] O.E. Garcia, J. Horacek, R.A. Pitts, A.H. Nielsen, W. Fundamenski, J.P. Graves, V. Naulin and J.J. Rasmussen, Plasma Phys. Control. Fusion **48**, L1 (2006).
- [15] O. Grulke, J.L. Terry, B. LaBombard and S.J. Zweben, Phys. Plasmas **13**, 012306 (2006).
- [16] B.D. Scott, Plasma Phys. Control. Fusion **45**, A385 (2003).
- [17] T.K. Chu, H.W. Hendel and P.A. Politzer, Phys. Rev. Lett. **19**, 1110 (1967).
- [18] H.W. Hendel, B. Coppi, F. Perkins and P.A. Politzer, Phys. Rev. Lett. **18**, 439 (1967).
- [19] H.W. Hendel, T.K. Chu and P.A. Politzer, Phys. Fluids **11**, 2426 (1968).
- [20] R.F. Ellis and R.W. Motley, Phys. Rev. Lett. **27**, 1496 (1971).

- [21] T. Klinger, A. Latten, A. Piel, G. Bonhomme, T. Pierre and T.D. de Wit, Phys. Rev. Lett. **79**, 3913 (1997).
- [22] O. Grulke, T. Klinger and A. Piel, Phys. Plasmas **6**, 788 (1999).
- [23] C. Schröder, O. Grulke, T. Klinger and V. Naulin, Phys. Plasmas **12**, 42103 (2005).
- [24] C.M. Franck, O. Grulke and T. Klinger, Phys. Plasmas **9**, 3254 (2002).
- [25] O. Grulke, S. Ullrich, T. Windisch and T. Klinger, Plasma Phys. Control. Fusion **49**, B247 (2007).
- [26] A.M. Keesee and E.E. Scime, Plasma Sources Sci. Technol. **16**, 742 (2007).
- [27] T. Windisch, O. Grulke and T. Klinger, Phys. Plasmas **13**, 122303 (2006).
- [28] V.I. Demidov, S.V. Ratynskaia, R.J. Armstrong and K. Rypdal, Phys. Plasmas **6**, 350 (1999).
- [29] R. Schrittwieser, C. Ionita, P. Balan, R. Gstrein, O. Grulke, T. Windisch, C. Brandt, T. Klinger, R. Madani, G. Amarandei and A.K. Sarma, Rev. Sci. Instrum. **79**, 083508 (2008).
- [30] H. Johnsen, H.L. Pécseli and J. Trulsen, Phys. Fluids **30**, 2239 (1987).
- [31] C. Schröder, O. Grulke, T. Klinger and V. Naulin, Phys. Plasmas **11**, 4249 (2004).
- [32] F. Brochard, T. Windisch, O. Grulke and T. Klinger, Phys. Plasmas **13**, 122305 (2006).
- [33] G.R. Tynan, C. Holland, J.H. Yu, A. James, D. Nishijima, M. Shimada and N. Taheri, Plasma Phys. Control. Fusion **48**, S51 (2006).
- [34] O.E. Garcia, N.H. Bian, V. Naulin, A.H. Nielsen and J.J. Rasmussen, Phys. Plasmas **12**, 090701 (2005).
- [35] A. Lichtenberg and M. Lieberman, *Regular and Chaotic Dynamics* (Springer, 1992).
- [36] C. Schöder, T. Klinger, D. Block, A. Piel, G. Bonhomme and V. Naulin, Phys. Rev. Lett. **86**, 5711 (2001).